Laser Flash Absorption Spectroscopy Study of Ferredoxin Reduction by Photosystem I in *Synechocystis* sp. PCC 6803: Evidence for Submicrosecond and Microsecond Kinetics

Pierre Q. Y. Sétif* and Hervé Bottin

C.E.A., Département de Biologie Cellulaire et Moléculaire, Section de Bioénergétique and CNRS URA 1290, C. E. Saclay, 91191, Gif sur Yvette, France

Received March 7, 1994; Revised Manuscript Received May 12, 1994®

ABSTRACT: The kinetics of reduction of soluble ferredoxin by photosystem I (PSI), both purified from the cyanobacterium *Synechocystis* sp. PCC 6803, were investigated by flash-absorption spectroscopy between 460 and 600 nm. Most experiments were made with isolated monomeric PSI reaction centers prepared with the detergent β-dodecyl maltoside. Analysis of absorption transients, in parallel at 480 and 580 nm and under several conditions, shows the existence of three different first-order components in the presence of ferredoxin ($t_{1/2} \approx 500$ ns, 20 μs, and 100 μs). A second-order phase of ferredoxin reduction is also present [$k = (2–5) \times 10^8$ s^{-1} at pH 8 and at moderate ionic strength]. Similar first-order kinetic components were found with membranes from *Synechocystis*, with dissolved crystals of trimeric PSI reaction centers from *Synechococcus*, and also when ferredoxin from *Synechocystis* is replaced by ferredoxin from *Chlamydomonas reinhardtii*. The three first-order phases exhibit similar, though not identical, spectra which are consistent with electron transfer from the [4Fe-4S] centers of PSI to the [2Fe-2S] center of ferredoxin and are all attributed to reduction of ferredoxin bound to PSI. At pH 8 and at moderate ionic strength, the dissociation constants associated with each of these components are also similar, with a global value varying between 0.2 and 0.8 μM in different cyanobacterial preparations. The presence of three exponential components is discussed assuming homogeneity of the two partners and using the estimated values for the shortest possible distance of approach of soluble ferredoxin from the different iron–sulfur centers of PSI. It is concluded that the 500-ns phase corresponds to electron transfer from either F_A^- or F_B^-, the terminal iron–sulfur acceptors of PSI, to ferredoxin and that the immediate electron donor to ferredoxin is reduced within less than 500 ns. The presence of at least two different types of PSI–ferredoxin complex, all competent in electron transfer, is also deduced from the kinetic behavior.

In oxygenic photosynthetic organisms, the reduction of soluble ferredoxin is mostly catalyzed by photosystem I (PSI).[1] This reaction is preceded by a multistep charge separation within the reaction center of PSI. This charge separation involves first the photochemical formation of the oxidized primary donor $P700^+$ (a dimer of chlorophyll molecules) and of the reduced primary acceptor. Electron transfer then proceeds along a series of electron acceptors, leading eventually to the reduction of one or both of the terminal acceptors F_A and F_B. These two acceptors are [4Fe-4S] centers which are both carried by a small subunit called PSI-C which is firmly associated to the core PSI reaction center. Ferredoxin is a small (10–11 kDa) and strongly acidic protein containing a [2Fe-2S] cluster. It exhibits a low redox potential [E_m = –0.412 V in the case of *Synechocystis* sp. PCC 6803 (Bottin & Lagoutte, 1992)] and is involved in the reduction of many different enzymes (Knaff & Hirasawa, 1991). Among the numerous partners of ferredoxin, ferredoxin-$NADP^+$ reductase (FNR) catalyzes the reduction of $NADP^+$. Ferredoxin also probably participates in cyclic electron transfer around PSI as well as in linear electron transfer. Four high-resolution structures have been determined for different cyanobacterial ferredoxins (Tsukihara et al., 1981, 1990; Rypniewski et al., 1991; Jacobson et al., 1993). The PSI reaction center is a large complex (approximately 300 kDa) containing at least 12 different subunits and about 100 chlorophyll molecules (Golbeck & Bryant, 1991). It is embedded in the photosynthetic membrane but also contains several protruding peripheral subunits. On the cytoplasmic side, cross-linking experiments using EDC suggested that the PSI-D subunit is involved in the docking of soluble ferredoxin (Zanetti & Meratti, 1987; Zilber & Malkin, 1988; Andersen et al., 1992a; Lelong et al., 1994), and a role for PSI-E in the interaction of PSI with ferredoxin (Andersen et al., 1992b; Sonoike et al., 1993; Rousseau et al., 1993) and FNR (Andersen et al., 1992b) has also been suggested. Both PSI-D and PSI-E subunits carry a net positive charge. A low resolution (6 Å) three-dimensional structure is now available for PSI from the cyanobacterium *Synechococcus* (Krauss et al., 1993).

When electron transfer occurs between different proteins, as it is the case for the system under study, it is thought to involve the formation of a transient complex. The three-dimensional structure of a complex between soluble electron transfer proteins which can reversibly associate has been recently obtained in the case of cytochrome *c* peroxidase and cytochrome *c* (Pelletier & Kraut, 1992) and in the case of methylamine dehydrogenase and amicyanin (Chen et al., 1992). However, the kinetic properties of electron transfer in such systems are not easy to study. In order to relate kinetic and structural properties, the complexes between photosynthetic reaction centers and their physiological partners are of special interest because electron transfer can be triggered by

* Author to whom correspondence should be addressed.

® Abstract published in *Advance ACS Abstracts*, June 15, 1994.

[1] Abbreviations: PSI, photosystem I; PSII, photosystem II; F_A, F_B, and F_X, the [4Fe-4S] centers of photosystem I; Fd, ferredoxin; FNR, ferredoxin-$NADP^+$ reductase; β-DM, β-dodecyl maltoside; OGP, octyl-β-D-glucopyranoside; DPIP, 2,6-dichlorophenolindophenol.

0006-2960/94/0433-8495$04.50/0 © 1994 American Chemical Society

light. The interaction between cytochrome c_2 and the reaction center of purple bacteria has thus been studied in many laboratories leading to some detailed understanding of molecular recognition (Tiede et al., 1993, and references therein). A related, though much less deeply characterized system is constituted by PSI and its soluble donors, plastocyanin or cytochrome c_6 (Bottin & Mathis, 1985; Hervas et al., 1994). The interaction between PSI-type reaction centers and soluble ferredoxins (or, in some cases, flavodoxins) represents another class of such complexes which should help in understanding the different interactions which govern recognition between electron-transfer proteins and the various parameters important for long-distance biological electron transfer processes. Despite the numerous interests of such a system, the functional properties of the electron transfer between PSI and ferredoxin have been investigated only recently (Hervas et al., 1992; Sonoike et al., 1993; Rousseau et al., 1993), well after some initial studies made with whole cells of the green alga *Chlorella* (Bouges-Bocquet, 1980). In the present work, we have undertaken to investigate further the kinetic features of the interaction between soluble ferredoxin and the PSI reaction center of the cyanobacterium *Synechocystis* 6803.

MATERIALS AND METHODS

Biological Samples. Different types of PSI reaction centers from *Synechocystis* 6803 were prepared after solubilization of the membranes by 1% (w/v) β-dodecyl maltoside (β-DM) (Rögner et al., 1990). Monomeric and trimeric PSI reaction centers were purified as described by Bald et al. (1992). Purification was stopped either after the centrifugation step on a sucrose density gradient or after the high-pressure liquid chromatography on a anion exchange column (Mono-Q, Pharmacia). In both cases, the PSI reaction centers were dialyzed against 20 mM Tricine/NaOH, pH 7.5, and 0.03% β-DM and concentrated by ultrafiltration (Centriprep 100, Amicon). A sample of further purified trimeric PSI, obtained after all steps described in Rögner et al. (1990), including the final purification through a HPLC hydroxyapatite column, was also provided by Dr. M. Rögner. Crystals of trimeric PSI from *Synechococcus* were provided by Dr. P. Fromme (Witt et al., 1992). The thylakoid membranes from *Synechocystis* used for absorption studies were obtained as described by Bottin and Lagoutte (1992). For all measurements, all samples studied were maintained in 0.03% β-DM. Ferredoxin from *Synechocystis* 6803 was prepared according to Bottin and Lagoutte (1992). Ferredoxin from *Chlamydomonas reinhardtii* was provided by Dr. J.-P. Jacquot (Schmitter et al., 1988). Chlorophyll concentration was determined according to Arnon (1949). The P700 content was calculated from photoinduced absorption changes at 820 nm assuming an absorption coefficient of 6500 M^{-1} cm^{-1} for $P700^+$ (Mathis & Sétif, 1981). The chlorophyll to P700 ratios were thus found to lie between 80 and 90 for the different types of isolated PSI reaction centers and between 103 and 110 for thylakoid membranes. The oxidized minus reduced difference spectrum of ferredoxin was measured in 33 mM Tris-HCl, pH 8.5, in the visible region. Ferredoxin was reduced by 5 mM sodium dithionite in the absence of redox mediators. An absorption coefficient of 9500 M^{-1} cm^{-1} for oxidized ferredoxin at 423 nm (relative maximum) (Tagawa & Arnon, 1968; Fee & Palmer, 1971) was assumed for calculating the differential absorption coefficients. The maximum of the difference spectrum was found at 428.5 nm ($\Delta\epsilon$ = 5000 ± 100 M^{-1} cm^{-1}).

Flash-Absorption Spectroscopy. Flash-induced absorption changes were measured at 296 K at 430 and 820 nm and in the 460–600-nm region. Excitation was provided by a ruby laser (Quantel, France; pulse energy ≈ 15 mJ; wavelength, 694.3 nm; duration, 6 ns; repetition rate, 0.1 Hz). A low repetition rate of the laser excitation was used for two reasons: first, low concentrations of exogenous donor (DPIP) are used so that reduction of $P700^+$ by reduced DPIP between two flashes ($t_{1/2} \approx 0.5$–1.0 s) is much slower than the processes under study. Second, reduced ferredoxin has to be fully reoxidized between two consecutive flashes: a halftime ≈ 30–100 ms was found for this process and is ascribed to reoxidation by dissolved oxygen. Laser flashes were saturating for PSI photochemistry. The measuring light was provided by a 200-W tungsten–halogen lamp, and the appropriate wavelength was selected with interference filters of 10-nm bandwidth placed before and after the (1 × 1 cm) square cuvette containing the sample. For measurements in the visible region, a shutter was placed just before the cuvette and was opened 1 ms before the actinic flash was fired, in order to avoid any actinic effect of the measuring light. A biased silicium photodiode (type S3590-05 from Hamamatsu) was used as the detector. The output signal was filtered and amplified using either the 7A13 Tektronix (DC-5 MHz) or 7A22 Tektronix (DC-1 MHz) plug-in amplifiers. The time resolutions thus obtained were 100 ns and 1 μs, respectively. The signals were recorded and digitized (Tektronix RTD710A) before storage on a PC microcomputer for further manipulation. Opening of the shutter led to some baseline distortion. This baseline was measured at each wavelength in the visible region with a cuvette containing water and was subtracted from the signals. In most cases, kinetic data were fitted to a multiexponential decay with a Marquardt least-squares algorithm. In a few cases, the same algorithm was also used for fitting data to the function of time $[A/(Bt + 1)]$ (second-order reaction with the two reactants having identical initial concentrations). The amplitudes of absorption changes were calibrated by measuring the flash-induced absorption change at 820 nm on every sample. After subtraction of the antenna and PSII components, the remaining signal is ascribed to $P700^+$, for which an absorption coefficient of 6500 M^{-1} cm^{-1} was assumed (Mathis & Sétif, 1981). For measuring signals which are not related to PSI photochemistry (triplet states of antenna molecules and PSII components), P700 was preoxidized before the laser flash excitation. This was done by preilluminating the sample with white light of a weak intensity (≈10 mW/cm^2; duration ≈ 2 s ending 1 s before the flash excitation) in the presence of 50 μM methylviologen and 0.5 mM sodium ascorbate. Under these conditions, the halftime of $P700^+$ reduction by ascorbate was found to be larger than 2 min.

RESULTS

In a previous flash-absorption study made at 480 nm with ferredoxin and PSI particles from *Synechocystis* 6803, reduction of soluble ferredoxin by PSI was reported to occur in tens of microseconds (Rousseau et al., 1993). The PSI particles were prepared after solubilization of the membranes with a mixture of the two detergents octyl β-D-glucopyranoside (OGP) and sodium cholate. Flat cuvettes (thickness 0.8 mm) were also used in order to restrict the sample volume. Such experimental conditions led to relatively poor results for the following reasons: (a) in the presence of ferredoxin, the OGP PSI particles form large aggregates. Moreover, it was found that the flash-induced absorption changes due to ferredoxin

reduction were followed by some scattering changes (Rousseau et al., 1993). This made the comparison of absorption changes between samples in the presence and absence of ferredoxin very difficult; (b) the reproducibility of absorption changes measurements was rather poor when recorded with flat cuvettes. This was due first to the difficulty of adjusting very precisely the concentrations of PSI in the control cuvette (no ferredoxin) and in the cuvette with ferredoxin, owing to the small volume of the sample, and second to the difficulty of positioning very reproducibly the flat cuvette, thus leading to some differences in the baselines between the two samples (with and without ferredoxin). In the present study, the reproducibility and the precision of the measurements are much higher than in the above study owing to the use of square cuvettes and PSI reaction centers prepared with β-dodecyl maltoside (see Materials and Methods). Neither aggregation nor light-induced scattering changes were observed with such reaction centers. In the following, PSI reaction centers were studied in their monomeric form except when indicated. Scattering and aggregation were also absent when working with membranes, as far as the experiments were performed in the presence of 0.03% β-DM. Except when indicated, the experiments were made under salts and pH conditions (30 mM NaCl, 5 mM $MgCl_2$, pH 8) which are not optimal for electron transfer but which appear more physiologically relevant than such optimal conditions (no monovalent cations, acidic pH, see below).

In isolated PSI, light excitation leads eventually to charge separation between $P700^+$ and the terminal acceptor (either F_A^- or F_B^-). This is followed by a charge recombination between these two species [see Ke (1973) for a review]. The latter process can be observed by monitoring the decay of $P700^+$ at 820 nm in a time scale of hundreds of milliseconds (Figure 1A, right part, curve 1). As previously described (Sonoike et al., 1993; Rousseau et al., 1993), addition of soluble ferredoxin leads to a much slower decay of $P700^+$ (Figure 1A, right part, curve 2). This behavior is expected when electron transfer proceeds from $(F_A, F_B)^-$ to ferredoxin, as $P700^+$ is then much more slowly reduced by low concentrations of the exogenous donor reduced DPIP. When recorded on a faster time scale (1 ms), the kinetic traces are identical whether ferredoxin is present or not (Figure 1A, left part, curves 1 and 2). Minor fast components with $t_{1/2} \approx 2$ and 14 μs are present in both cases. They can be most probably ascribed to some triplet states of antenna chlorophylls as they are no longer observable when using subsaturating laser intensities. However, a high intensity of laser excitation was preferred throughout this study in order to ensure an almost complete saturation of PSI photochemistry. This was found to be necessary for comparing in a reliable manner the absorption changes between samples which were identical except for the absence or the presence of ferredoxin. In accordance with the above interpretation, the fast transients are still present when $P700^+$ is preoxidized before the laser flash excitation. This preoxidation was performed in two different ways, either in the presence of potassium ferricyanide (not shown) or in the presence of methylviologen and with a small amount of sodium ascorbate (and without DPIP) (Figure 1, curves 3). Under the latter conditions, the sample was preilluminated just before the laser flash in order to photooxidize P700 (see Material and Methods). Whenever antenna signals were to be subtracted, this last method was found to be much more reliable than chemical oxidation by ferricyanide. This is due to the fact that the decay of antenna triplet states (arising from either carotenoids or chlorophylls, or both) was slightly

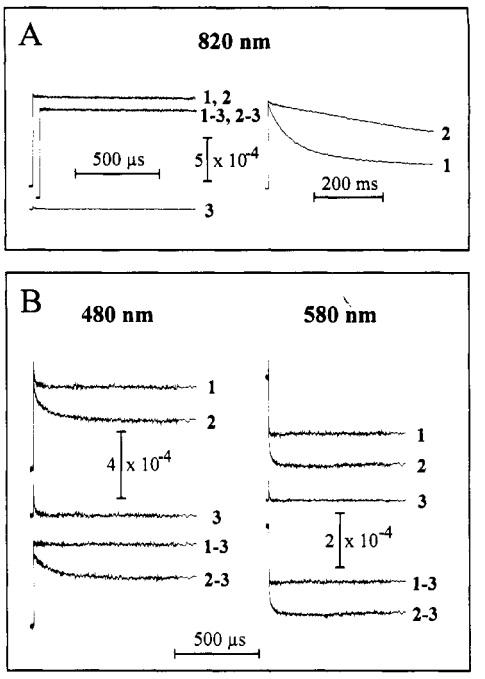

FIGURE 1: Flash-induced absorption changes measured with PSI monomers from *Synechocystis* 6803 at 820 (part A), 480, and 580 nm (part B) with or without soluble ferredoxin from *Synechocystis*. The PSI reaction centers (absorbance at 679.0 nm = 0.93) were suspended in 20 mM Tricine, pH 8, in the presence of 0.03% β-DM, 30 mM NaCl, and 5 mM $MgCl_2$. (Curves 1) + 6 μM DPIP (no ferredoxin) + 1 mM sodium ascorbate. (Curves 2) + ferredoxin (concentration of 2.17 μM) + 1 mM sodium ascorbate + 6 μM DPIP. (Curves 3) + 50 μM methylviologen + 0.5 mM sodium ascorbate (no ferredoxin, no DPIP). For curves 3, the sample was preilluminated for 2 s with a weak light ending 1 s before the laser flash. Traces are averages of eight experiments (820 nm) or 32 experiments (480 and 580 nm). From the curves 1–3 and 2–3 at 820 nm, the PSI concentration is estimated to be 0.161 μM.

accelerated by the addition of ferricyanide, whereas the initial amount of these triplet states becomes larger (possibly due to disconnection of some antenna pigments after oxidation of some chlorophylls by ferricyanide). After having subtracted these antenna signals from the original decay curves, it appears that the decay of $P700^+$ is negligible on a 1-ms time scale (Figure 1A, curves 1–3 and 2–3).

Comparison of absorption spectra of oxidized [2Fe-2S] and [4Fe-4S] clusters indicates that the [2Fe-2S] species have a larger absorbance than the [4Fe-4S] species above 480 nm and exhibit a significant absorbance up to 600 nm. This is also true for the differential (oxidized minus reduced) spectra of the two species. As a result, electron transfer from $(F_A, F_B)^-$ to the [2Fe-2S] cluster of ferredoxin should be accompanied by an absorbance decrease in this wavelength region. This property has been used in two previous studies reporting laser flash-induced reduction of ferredoxin by PSI monitored at 480 nm (Hervas et al., 1992; Rousseau et al., 1993). The kinetic traces observed with PSI reaction centers in the absence and in the presence of ferredoxin (2.2 μM for a PSI concentration of 0.16 μM) are shown in Figure 1B at 480 and 580 nm (curves 1 and 2, respectively). Similarly to the measurements at 820 nm, the initial absorption changes observed in the absence of ferredoxin are followed at both wavelengths by some fast decay components due to antenna triplet states. These transient signals can be recorded separately with P700 preoxidized before the flash excitation (curves 3). After subtraction of the antenna signals (curves 1–3 at 480 and 580 nm), it appears that there is no significant absorption change during the first millisecond following flash

excitation. When the kinetic traces recorded in the presence of ferredoxin (curves 2) are corrected for the antenna components in the same manner (curves 2–3), two distinctive features emerge immediately: (1) the initial absorption change in the presence of ferredoxin is found below that observed in the absence of ferredoxin. As the above signals were recorded with a microsecond time resolution, this may indicate the presence of a faster unresolved component of ferredoxin reduction. This component will be referred in the following as the submicrosecond component. (2) Some decay components are visible in the microsecond range, in accordance with a previous report (Rousseau et al., 1993). The submicrosecond component escaped observation in the latter report due to the experimental conditions (see above) and to the fact that the first study was done at 480 nm, where the relative size of the submicrosecond component is smaller. Kinetics of absorption changes were measured in the same way with thylakoid membranes of *Synechocystis*, with identical concentrations of PSI and ferredoxin. Results are very similar to those obtained with isolated PSI reaction centers, except for larger signals not related to PSI photochemistry, as it can be expected from the presence of PSII in the membranes. After subtraction of the PSII and antenna signals, the kinetics and the amplitudes of the signals were found to be very close to those shown in Figure 1 for PSI particles (see also Figure 2).

Figure 2 shows the differences between the transient signals observed at 480 and 580 nm in the presence and in the absence of ferredoxin (curves c corresponding to the differences between curves 1 and 2 of Figure 1). This approach, which allows us to put forward directly the effect of ferredoxin, is fully justified in the present case as no transient is observed on a millisecond time scale in the absence of ferredoxin (see curves 1–3 in Figure 1). The two traces exhibit significantly different microsecond kinetic profiles, with a decay globally slower at 480 nm than at 580 nm. This indicates the presence of at least two microsecond phases ($t_{1/2} \approx 20$ and 100 μs), as it can be also seen from the residuals of the fits with one and two exponential decay phases (traces 1 and 2 of Figure 2). Moreover, these two phases exhibit different spectra. The corresponding signals observed with PSI membranes (curves b) exhibit the same biphasic character but the decay is slightly faster (16 and 85 μs). The question arises whether these two microsecond components are first- or second-order reactions. Three independent approaches, described in the following, were used in order to answer this question. All of them support first-order processes for both microsecond components:

(1) The kinetic behavior was studied at different concentrations of ferredoxin. The amplitudes of the two phases change with ferredoxin concentration without modification of their rates.

(2) The absorption changes were studied in the presence of 35% glycerol (v/v; 44% w/w) with concentrations of PSI and ferredoxin identical to those used in its absence (curves a). The 4.5-fold increase in viscosity thus obtained is expected to slow down second-order processes limited by diffusion of the two reactants. As in the absence of glycerol, comparison of the kinetics at 480 and 580 nm on a 400-μs time scale shows clearly the presence of two microsecond components (curves a of Figure 2). Fitting the observed decay with two exponential phases gives approximately the same rates as in an aqueous medium ($t_{1/2} \approx 20$ and 135 μs). However, the total amplitude of the signal is smaller, indicating that glycerol decreases the affinity of ferredoxin for PSI (see Table 2). Higher amounts of glycerol (50 and 70% v/v) were also tested and were found to decrease dramatically the affinity of ferredoxin for PSI.

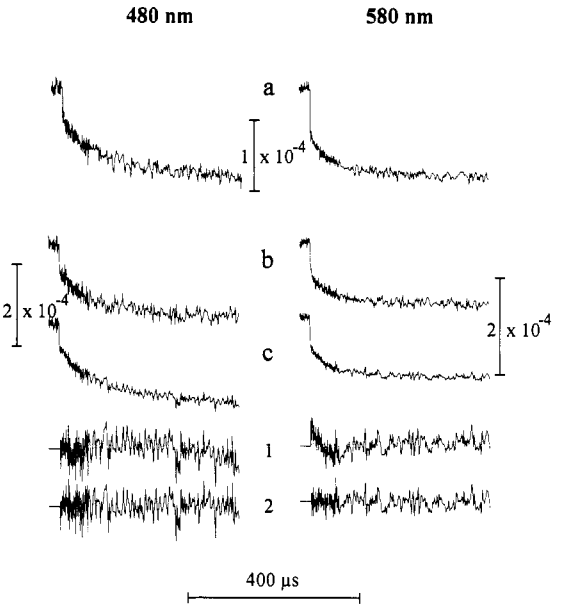

FIGURE 2: Differences between flash-induced absorption changes measured in the presence and in the absence of soluble ferredoxin at 480 and 580 nm. These differences were obtained from kinetic traces similar to curves 1 and 2 of Figure 1 [difference (2 – 1)]. (a) PSI monomers in the presence of 35% glycerol v/v (44% w/w). (b) Membranes from *Synechocystis* (no glycerol). (c) PSI monomers (no glycerol). The measurements were made in 20 mM Tricine, pH 8, in the presence of 0.03% β-DM, 1 mM sodium ascorbate, 30 mM NaCl, 5 mM $MgCl_2$, and DPIP (6 μM in the absence of glycerol and 22 μM in its presence). For all three cases, the PSI and the ferredoxin concentrations are, respectively, 0.16 and 2.17 μM. The original traces used for obtaining the differences were averages of 32 (for b and c) or 64 (for a) experiments. The lower traces 1 and 2 are the residuals (multiplied by 3) from a global fit of the two curves c at 480 and 580 nm. Fitting was made with either one (curves 1) or two (curves 2) exponential components. An offset parameter was used in addition to the exponential phases in order to take into account the longer-lived absorbance change. The halftimes are 63 μs in the one-component fit and 20 and 103 μs in the two-component fit. For the two-component fit, the amplitudes of the submicrosecond component (unresolved here and estimated as an initial amplitude) and the 20- and the 103-μs components are (0.48×10^{-4}, 0.45×10^{-4}, 0.92×10^{-4}) at 480 nm and (0.50×10^{-4}, 0.44×10^{-4}, 0.32×10^{-4}) at 580 nm.

(3) The measurement of the second-order rate constant was attempted under similar conditions of pH and salts concentrations. This measurement cannot be performed under pseudo-first-order conditions (large excess of ferredoxin compared to PSI) due the high affinity of ferredoxin for PSI (dissociation constant $K_d < 1$ μM; see below). Therefore low concentrations of both partners were used in order to get a significant contribution from second-order processes. Identical concentrations of the two reactants must also be used if data are to be fitted with an analytical function. However these concentrations must be high enough for an efficient electron transfer to ferredoxin. If it were not the case, the recombination reaction between $P700^+$ and $(F_A, F_B)^-$ would compete with reduction of ferredoxin. In addition, reoxidation of reduced ferredoxin, most probably by dissolved oxygen, is occurring under our experimental conditions with a $t_{1/2}$ in the 30–100-ms range (not shown). Therefore reduction of ferredoxin must be significantly faster than these two processes, at least during the 10-ms period during which the fitting was performed. A concentration of 0.25 μM for both partners was thus found to be optimal for the measurement of the second-order rate constant. Data were fitted during the first 10 ms following flash excitation, neglecting both the recombination of $P700^+$ and $(F_A, F_B)^-$ and the reoxidation of reduced ferredoxin. Second-order rate constants of 2 to 5×10^8 M^{-1}

Table 1: Second-Order Rate Constants for Reduction of Ferredoxin by PSI Determined under Different Conditions

experimental conditions	amplitude of second-order component (in percent of the total signal due to ferredoxin reduction)	rate constant ($\times 10^8$ M^{-1} s^{-1})
[PSI] = [ferredoxin] = 0.25 μM: pH 8, 30 mM NaCl, 5 mM $MgCl_2$	60 ± 10%	3.5 ± 1.5
[PSI] = 0.18 μM; [ferredoxin] = 2.02 μM; pH 8, 100 mM NaCl	50 ± 10%	2.5 ± 0.6
[PSI] = 0.18 μM; [ferredoxin] = 1.93 μM; pH 8, 250 mM NaCl	80 ± 10%	1.5 ± 0.3

Table 2: Properties of the PSI–Ferredoxin Electron Transfer Complexes for Different PSI Preparations and Soluble Ferredoxins[a]

system under study	dissociation constant (μM)	presence of three first-order kinetic components of ferredoxin reduction
PSI monomer/SDG	0.39/0.43[b]	+
PSI monomer/SDG + HPLC	0.36/0.63[b]	nd[c]
PSI trimer/SDG	0.22	nd
PSI trimer/SDG + HPLC	0.29	nd
PSI trimer/SDG + HPLC + HX[d]	0.83	nd
membranes from *Synechocystis* 6803	0.46	+
PSI monomer/SDG; 35% glycerol	2.5	+
PSI monomer/SDG; ferredoxin from *Chlamydomonas reinhardtii*[e]	1.8	+
dissolved crystals of PSI trimers from *Synechococcus*[f]	0.33	+

[a] The dissociation constants were measured under conditions similar to those described in the legend to Figure 4. All measurements were made in 20 mM Tricine, pH 8, 30 mM NaCl, and 5 mM $MgCl_2$ in the presence of 0.03% β-DM. Except where indicated, the measurements were made with PSI reaction centers and ferredoxin from *Synechocystis* 6803 in the absence of glycerol. Whereas some reaction centers were purified in a single step by a sucrose density gradient (SDG), one or two further steps were used in some other cases (anion-exchange chromatography by HPLC, denoted HPLC followed in one case by an hydroxyapatite HPLC column, denoted HX). [b] Two different preparations. [c] nd, not determined. [d] Reaction centers prepared by Dr. M. Rögner. [e] Ferredoxin given by Dr. J.-P. Jacquot. [f] Crystals given by Dr. P. Fromme.

s^{-1} were found (Table 1). The upper limit of the second-order rate constant thus found would give a $t_{1/2}$ of about 630 μs for the experiments depicted in Figures 1 and 2 (assuming a pseudo-first-order reaction, the concentration of ferredoxin being much higher than that of PSI), which is much slower than the decay of the slower phase ($t_{1/2} \approx 100$ μs).

The above considerations strongly support the conclusion that both the 20- and 100-μs phases correspond to first-order processes. Though the presence of these two components has been generally observed (see Table 2), their halftimes are changing somewhat from one PSI preparation to another. In all types of PSI reaction centers from *Synechocystis* 6803 that were studied, these halftimes were found to lie between 10 and 30 μs for the faster component and between 60 and 140 μs for the slower one.

The submicrosecond component was further studied with a higher time resolution (100 ns). Figure 3A exhibits the flash-induced absorbance changes observed at 580 nm in the absence (curve 1) or in the presence (curve 2) of ferredoxin. The two kinetic traces can be superimposed during the first 200 ns following flash excitation, and a lag is visible in the difference between the two curves (2 – 1). Evidence for a lag is better seen when the same difference is plotted on a shorter time scale together with the absorbance change at 820 nm monitoring the instrument limited rise of $P700^+$ (Figure 3B). This lag receives a simple interpretation if one assumes that the submicrosecond decay following the lag is due to ferredoxin reduction and that the immediate donor to ferredoxin is reduced in a few hundreds of nanoseconds. This last assumption is consistent with a previous report where it was proposed that electron transfer to either F_A or F_B proceeds with a halftime of 200 ns in cyanobacterial reaction centers (Sétif & Brettel, 1993). The difference (2 – 1) shown in Figure 3 was fitted either with two or with three exponential components, without taking into account the instrument limited rise of the setup. Fitting with two components (halftimes of 530 ns and 22 μs) leads to a poor fit just after the flash (residuals: trace b; the residuals at later times are negligible), as the lag is not properly taken into account. Fitting with three components was performed by fixing the halftime of one phase to 200 ns in order to account for the reduction of the immediate donor to ferredoxin. The two other components were found with $t_{1/2}$ of 500 ns and 22 μs (residuals: trace a; see the legend to Figure 3). Whereas the 22-μs component accounts for the microsecond decay phases described above, the 500-ns phase is attributed to the fastest phase of ferredoxin reduction. Similar experiments were also performed at 580 nm in the presence of 35% glycerol, and the halftime of the fastest component was also found to be around 500 ns.

The three different phases that appear upon ferredoxin addition ($t_{1/2} \approx 500$ ns, 20 μs, and 100 μs) are being further characterized, and their properties will be described in a forthcoming paper. However a qualitative overview of these properties can be already given: (1) the kinetic profile of the differential (in the presence minus in the absence of ferredoxin) absorption changes is weakly dependent upon the ferredoxin concentration. When the amplitude of each phase is analyzed independently considering a simple equilibrium between PSI and ferredoxin, the dissociation constants corresponding to the three phases are thus found to be similar within a factor of 2. (2) The decay-associated spectra of the three components have been characterized between 460 and 600 nm. Whereas the spectra of the 500-ns phase (determined generally as an unresolved submicrosecond component in experiments performed with a microsecond time resolution) and of the 20-μs phase appear to be similar, they are both somewhat different from the spectrum of the 100-μs phase. At this point, it should be stressed that the reliability of the spectral analysis strongly depends upon the precision with which the halftimes of the two microsecond components are determined. As the halftimes of these components are not so different, a slight error in their estimation leads to significant modifications of the decay-associated spectra. Thus, at the moment, a minimal conclusion that can be drawn is that the spectra of the 20- and 100-μs phases are surely different (as can be seen directly from examination of Figure 2) whereas we cannot ascertain that the 500-ns and 20-μs phases have identical spectra. We also observed some properties common to all three spectra: their amplitude is positive between 480 and 600 nm, and their

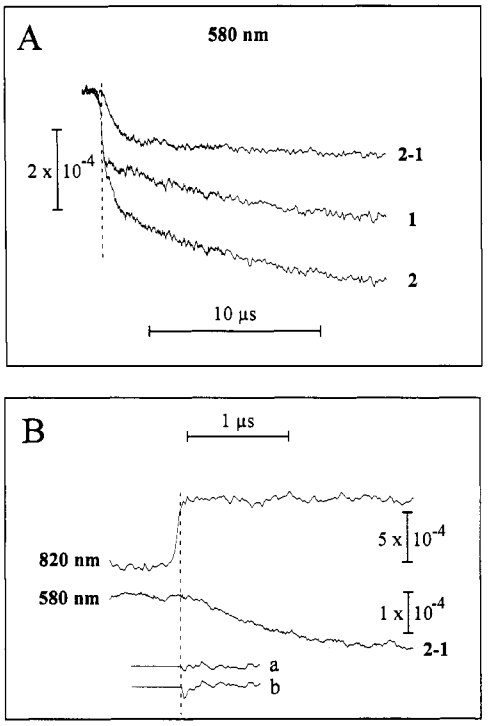

FIGURE 3: (A) Flash-induced absorption changes measured with PSI monomers at 580 nm with a 100-ns time resolution in the absence (curve 1) or in the presence of 4.6 μM ferredoxin (curve 2). The PSI reaction centers (absorbance at 679.0 nm = 2.02; concentration of 0.35 μM) were suspended in 20 mM Tricine, pH 8, in the presence of 0.03% β-DM, 1 mM sodium ascorbate, 8 μM DPIP, 30 mM NaCl, and 5 mM $MgCl_2$. Traces are the average of 128 experiments. The difference between the two transient kinetics is shown as curve (2 – 1). An expanded part of this difference is shown in panel B together with the absorbance change measured at 820 nm under conditions of weak laser light excitation (about 30% of the reaction centers oxidized). Curve (2 – 1) was fitted (time zero was taken at the dashed vertical line) with either two exponential components or three components with one component fixed at a halftime of 200 ns (plus an offset parameter in both cases). The corresponding residuals (multipled by 3) are shown as curves a (three components) and b (two components). The parameters of the three component fit are $(t_{1/2})_1$ = 200 ns (fixed), $A_1 = -1.00 \times 10^{-4}$, $(t_{1/2})_2$ = 495 ns, $A_2 = 2.21 \times 10^{-4}$, $(t_{1/2})_3$ = 22 μs, $A_3 = 1.11 \times 10^{-4}$, offset = -2.31×10^{-4}, and initial amplitude = 0.01×10^{-4}. The dashed vertical lines are drawn for helping in the comparison of the time dependence of the different signals.

general shape in this region is fully consistent with electron transfer from $(F_A, F_B)^-$ to ferredoxin. It should be also emphasized that, under the conditions tested so far, none of the three phases is of negligible amplitude: at any wavelength between 480 and 600 nm, the amplitude of any of the three phases represents at least 20% of the total amplitude corresponding to the three phases.

From this point, only some global properties of the absorption changes induced by the presence of ferredoxin will be described. This appears to be a reasonable approach as the characteristics of the three exponential components, though not identical, are rather similar. Except when indicated, the following results describe the signals measured 300 μs after the flash on decay curves corresponding to the difference between samples in the presence and in the absence of ferredoxin (respectively similar to curves 2 and 1 of Figure 1). At this time, the first-order processes have almost entirely ended, and the contribution from a second-order process is small. Figure 4 shows the signal amplitudes observed at 480 and 580 nm at different ferredoxin concentrations. These data were fitted assuming a simple binding equilibrium between PSI and ferredoxin. Values of 0.39 and 0.40 μM for the dissociation constants

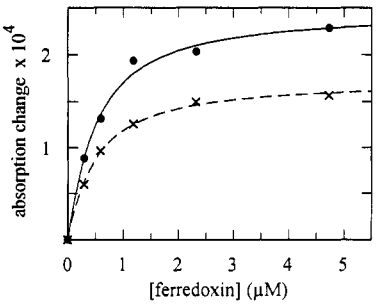

FIGURE 4: Dependence of the flash-induced absorption changes measured 300 μs after the flash on the ferredoxin concentration. The signal was measured at 480 nm (closed circles) and 580 nm (crosses) on curves similar to those shown in Figure 2 (signal in the presence minus signal in the absence of ferredoxin). Signals at both wavelengths are negative, and absolute values are shown here. Monomeric PSI reaction centers were suspended in the same medium as in Figure 3 (concentration between 0.195 and 0.191 μM due to addition of aliquots of a concentrated solution of ferredoxin). Assuming that the observed signal corresponds to bound ferredoxin, the two curves were fitted considering a simple binding equilibrium between free and bound ferredoxin. For fitting the data, the PSI concentration was assumed to have a constant value of 0.193 μM. The dissociation constants K_d and the maximum amplitude A_{max} of the signals (100% binding) were adjustable parameters. The parameters found were K_d = 0.39 μM and $A_{max} = 2.48 \times 10^{-4}$ at 480 nm and K_d = 0.40 μM and $A_{max} = 1.73 \times 10^{-4}$ at 580 nm.

were thus calculated for the signals measured at 480 and 580 nm, respectively.

After the reduction of ferredoxin and before the reduction of $P700^+$ by exogenous donors, the redox state of the system under study is $(P700^+ - Fd^-)$ (Fd for soluble ferredoxin). This should be the predominant redox state at 300 μs after the flash, except for a small proportion of reaction centers where electron transfer from $(F_A, F_B)^-$ to Fd has not yet occurred. The contribution of $P700^+$ needs to be subtracted for obtaining the spectrum corresponding to ferredoxin reduction. The difference spectrum of P700 was determined in the 460–600-nm region using methylviologen as an electron acceptor. Under such conditions, it has been shown that $(F_A, F_B)^-$ can rapidly transfer an electron to methylviologen, which is then very rapidly reoxidized by dissolved oxygen (Ke, 1973). Such kinetics of $(F_A, F_B)^-$ reoxidation are shown at 480 nm in the inset of Figure 5 (curve a in the presence of 50 μM methylviologen: $t_{1/2} \approx 1.6$ ms; curve b without exogenous acceptor). Assuming an absorption coefficient of 6500 M^{-1} cm^{-1} for $P700^+$ at 820 nm (Mathis & Sétif, 1981), the value of the differential absorption coefficient corresponding to the one-electron reduction of (F_A, F_B) is found to be 2500 ± 100 M^{-1} cm^{-1} at 480 nm. This coefficient was also determined to be about 8000 ± 300 M^{-1} cm^{-1} at 430 nm. The $(P700^+ - P700)$ difference spectrum was obtained in the 460–600-nm region on curves similar to curve a of Figure 5 by measuring the amplitude of the absorbance change at 10 ms after the flash. It was subtracted from the absorbance change measured 300 μs after the flash on a sample containing 2.18 μM ferredoxin (similar to curves 2 in Figure 1) and an identical PSI concentration (redox state $P700^+ - Fd^-$). The difference between these two spectra should therefore correspond solely to the reduction of ferredoxin. This spectrum is plotted in Figure 5 (closed circles, photochemical spectrum) together with the difference spectrum of isolated ferredoxin (continuous curve, chemical spectrum; see Material and Methods). The overall shape of the two spectra is similar, as can be expected if the transient signals correspond to reduction of ferredoxin by PSI. However, the photochemical spectrum is generally of smaller amplitude (except at 460 nm) than the chemical

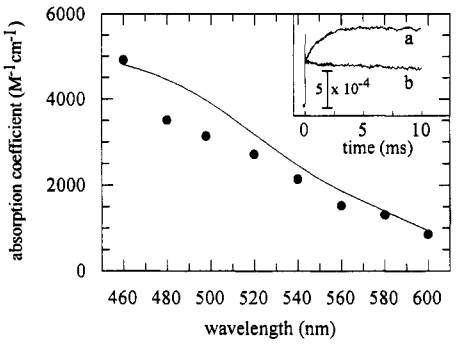

FIGURE 5: Spectrum of the flash-induced absorption changes due to ferredoxin photoreduction by PSI measured between 460 and 600 nm. The spectrum (closed circles) corresponds to the difference between (1) the signal measured at 10 ms after the flash in a PSI sample containing 50 μM methylviologen and no ferredoxin (0.187 μM PSI; redox state $P700^+$, all acceptors oxidized; similar to curve a of the inset) and (2) the signal measured 300 μs after the flash in a PSI sample containing 2.18 μM ferredoxin [0.187 μM PSI; other conditions as in Figure 3; redox state ($P700^+$, Fd^-) in about 87% of the reaction centers, redox state ($P700^+$, $(F_A, F_B)^-$) in about 13% of the reaction centers; see text for details]. All curves are averages of 32 experiments. Calibration of the vertical scale was made by measuring the absorption change at 820 nm on the same samples and assuming an absorption coefficient of 6500 M^{-1} cm^{-1} for $P700^+$ at 820 nm. This spectrum is shown with the difference spectrum corresponding to the chemical reduction of ferredoxin (full line). (Inset) Flash-induced absorption changes measured at 480 nm either in the absence or in the presence of 50 μM methylviologen (0.187 μM PSI; no ferredoxin, other conditions as in Figure 3).

spectrum. This can be due to some extent to the fact that ferredoxin reduction is only partial at 300 μs. Assuming a dissociation constant of 0.395 μM and a second-order rate constant of 3.5×10^8 M^{-1} s^{-1} for ferredoxin reduction, it can be calculated that electron transfer to ferredoxin has occurred in about 87% of the reaction centers at this time (the subpopulation of PSI being complexed to ferredoxin, which amounts to 84% of total PSI, is considered to have undergone full reduction of ferredoxin, and 19% of the remaining PSI, which makes 3% of the total, has reduced ferredoxin by a second-order reaction at 300 μs after the flash). The larger deviation between the two spectra that is observed at 480 and 500 nm is not understood at the moment.

The properties of electron transfer from PSI to ferredoxin were also studied under different conditions of ionic strength and pH (Figures 6 and 7), with isolated monomeric PSI reaction centers as well as with thylakoid membranes. The measurements were made at 580 nm, a wavelength at which it is easier to evaluate precisely the amount of the submicrosecond phase. Throughout these studies, it was found that the relative proportions of the submicrosecond and microsecond components were fairly constant so that it is sufficient to describe the global dependence (submicrosecond + microsecond phases) of the absorption changes due to ferredoxin addition. The amplitude of the signals was measured 300 μs after the flash, as described above, and corresponds essentially to the PSI–ferredoxin intracomplex electron transfer. As electrostatic interactions may play an essential role in the interaction between PSI and ferredoxin (Hervas et al., 1992; Zanetti & Merati, 1987; Lelong et al., 1994), changing the ionic strength could provide some valuable information. The results of such experiments are shown in Figure 6A where NaCl concentration is changed from 0 to 100 mM at pH 8. As it has been previously reported (Hervas et al., 1992), an optimal concentration of NaCl is found for electron transfer (about 10 and 50 mM for isolated PSI and membranes, respectively). Such a behavior has also been described in

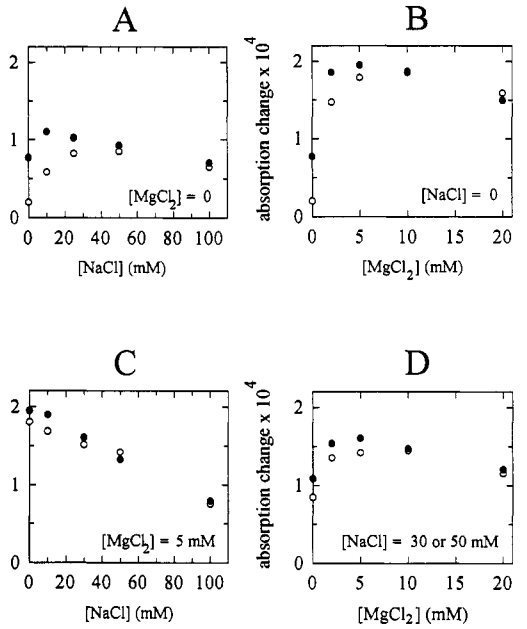

FIGURE 6: Salt dependence of the flash-induced absorption changes due to ferredoxin photoreduction by PSI. The signal was measured at 580 nm 300 μs after the flash on curves similar to those shown in Figure 2 (signal in the presence minus signal in the absence of ferredoxin; both are average of 32 experiments). Signals are negative, and absolute values are shown here. Monomeric PSI reaction centers (closed circles) or membranes (open circles) were suspended in 20 mM Tricine, pH 8, in the presence of 0.03% β-DM, 1 mM sodium ascorbate, and 6 μM DPIP. For both measurements with isolated reaction centers and membranes, the PSI concentration lies between 0.29 and 0.28 μM, and the ferredoxin concentration lies between 1.07 and 1.03 μM (due to the dilution effects when adding salts). Data were normalized by a multiplicative factor to a PSI concentration of 0.285 μM. (A) no $MgCl_2$. (B) no NaCl. (C) 5 mM $MgCl_2$. (D) 30 mM NaCl (isolated PSI) or 50 mM NaCl (membranes).

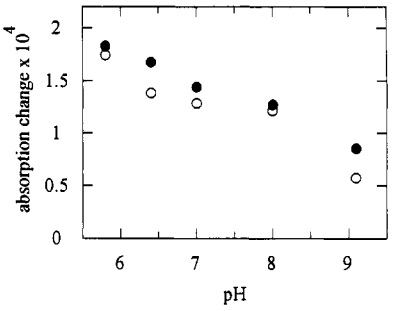

FIGURE 7: pH dependence of the flash-induced absorption changes due to ferredoxin photoreduction by PSI. Measurements are made at 580 nm as described in the legend to Figure 6. Monomeric PSI reaction centers (closed circles) or membranes (open circles) were suspended in 20 mM buffers in the presence of 0.03% β-DM, 1 mM sodium ascorbate, 30 mM NaCl, 5 mM $MgCl_2$, and 6 μM DPIP. The different buffers used were MES, pH 5.8 and 6.4, MOPS, pH 7.0, Tricine, pH 8.0, and borate, pH 9.1.

other systems and was considered as an evidence for the existence of an optimal range of electrostatic forces favoring electron transfer (Hurley et al., 1993, and references therein). Hervas and colleagues (1992) interpreted their results as an effect of ionic strength on the rate constant of electron transfer though it is likely that, in their case, the binding affinity was affected as well. In the present study, the first-order kinetics were not found to be strongly disturbed by changing the concentration of salts or the pH (less than 50% modification of the halftimes when compared to 20 and 100 μs). Therefore, the signal dependencies shown here and in Figure 7 reflect mostly modifications in the affinity of ferredoxin for PSI. The

decrease in binding constant at high ionic strength is expected for two partners of opposite charges, as is the case for the present reaction. An explanation for the affinity increase at low ionic strength is less straightforward. It was suggested earlier that, when electrostatic forces are too strong (at low ionic strength), the two partners could be locked in an unfavorable relative position. With isolated PSI, fast electron transfer is still occurring in the preformed complexes under conditions of low ionic strength, and the nonoptimal binding could be due to some negatively charged residues of PSI close to the docking site.

The second-order rate constant was also evaluated at high ionic strength. Contrary to the measurement of this rate constant under low salts conditions, it was possible to make this study under pseudo-first-order conditions (Table 1), as ferredoxin in large excess over PSI could be used without having most of PSI reaction centers complexed to ferredoxin. The results indicate a decrease in the second-order rate constant by a factor of almost 2 when the NaCl concentration changes from 100 to 250 mM.

A specific role for the Mg^{2+} cation has been previously reported in the interaction between PSI and ferredoxin (Hervas et al., 1992). In agreement with these observations, the affinity of ferredoxin for PSI increases when $MgCl_2$ is added in the presence of NaCl at a concentration that was found to be optimal for NaCl when it was added alone (Figure 6D). Moreover, the largest affinity at pH 8 is observed in the presence of only Mg^{2+} ($\approx$5 mM) and in the absence of NaCl (Figure 6B,C). It has been previously speculated that dications could serve to enhance collisions between PSI and ferredoxin by neutralizing negative charges on PSI via coordination rather than just electrostatic screening (Hervas et al., 1992). Our interpretation for the ionic strength dependency of the affinity is in line with this suggestion as divalent cations may play a role as bridges between negatively charged residues carried by the two partners.

It should be noted also that the efficiency of ferredoxin reduction at low ionic strength is much smaller in membranes than in isolated PSI. This suggests the presence in the membranes of some ferredoxin binding sites competing efficiently with PSI only at low ionic strength. The pH dependence of the 300-μs signal is shown in Figure 7. In line with previous observations (Hervas et al., 1992), this signal decreases monotonically when pH is increased from 5.8 to 9.1 (in the presence of 30 mM NaCl and 5 mM $MgCl_2$).

The presence of a submicrosecond phase together with a phase with a halftime comprised between 10 and 30 μs was found for all types of cyanobacterial PSI that we studied so far. The presence of two different microsecond components was not always tested reliably but was ascertained in the most important cases (Table 2). Table 2 shows also the list of the different systems which were tested together with the "global" dissociation constants that were measured as described in the legend to Figure 4. These include many different preparations of reaction centers from *Synechocystis* 6803. These reaction centers were prepared in their monomeric or trimeric forms at different degrees of purity (see Material and Methods). The dissociation constants measured for the PSI–ferredoxin complex are between 0.22 and 0.83 μM. Within each type of reaction center (trimer or monomer), the affinity of ferredoxin for PSI seems to slightly decrease when further purification steps are used to improve the purity of the preparation. For a given number of purification steps, the affinity appears to be slightly higher for the trimer than for the monomer. However, these variations are rather small and should be interpreted with caution. More interestingly, the dissociation constant measured in membranes from *Synechocystis* has about the same value as in isolated monomeric PSI. This strongly suggests that there is no significant perturbation brought to PSI reaction centers during their isolation with regard to the interaction with ferredoxin. However, it should be remembered that the experiments with membranes were made in the presence of 0.03% β-DM. As noted above, the "global" affinity decreases considerably in the presence of 35% glycerol ($K_d \approx 2.5$ μM). Such a decrease in the binding constant in the presence of glycerol has been already observed in the case of cytochrome c_2 and the reaction center of *Rhodobacter sphaeroides* (Venturoli et al., 1993). There are two types of interactions between glycerol and proteins (Gekko & Timasheff, 1981; Timasheff & Arakawa, 1989). Whereas the preferential hydration of proteins in glycerol–water mixtures due to the so-called solvophobic effect could favor the formation of complexes, the affinity of glycerol for polar regions of proteins should have an opposite effect. Our observations are consistent with the last type of interaction being dominant for the system under study.

We also studied electron transfer from *Synechocystis* PSI to soluble ferredoxin which was purified from the green alga *Chlamydomonas reinhardtii* (Schmitter et al., 1988). The kinetics of ferredoxin reduction are very close to those described above as three different phases of electron transfer were found (one submicrosecond phase, 29 μs and 130 μs). However, the global dissociation constant was found to be significantly higher (about 1.8 μM) than with ferredoxin from *Synechocystis*. This may be related to the fact that the global negative charge of the *Chlamydomonas* ferredoxin is smaller than that of ferredoxin from *Synechocystis*. Electron transfer from *Synechococcus* PSI to ferredoxin from *Synechocystis* was also studied. In order to ensure the highest standard of homogeneity that was attainable for PSI reaction centers, these were obtained from dissolved crystals of PSI trimers (gift from Dr. P. Fromme). In that case, three first-order components were also found for ferredoxin reduction with halftimes of <1, 14, and 80 μs. The dissociation constant is also comparable (0.33 μM) to that found with PSI from *Synechocystis*.

DISCUSSION

Some results on electron transfer between PSI and ferredoxin from *Synechocystis* were previously reported (Rousseau et al., 1993). There are some discrepancies between these former results and the present data. The second-order rate constant for reduction of ferredoxin was first estimated to be about 1×10^9 s^{-1}, whereas a value of $(2–5) \times 10^8$ s^{-1} is found in the present work, under similar pH and salt conditions. The amount of first-order reactions in the process of ferredoxin reduction was also underestimated. We regard the present analysis as much more reliable, in view of the various experimental difficulties which were encountered in the initial study and which are now eliminated. It was also reported that the size of the transient signal observed at 480 nm and ascribed to ferredoxin reduction corresponded to only 40% of what is expected for reduction of ferredoxin by 100% of the PSI complexes. For this calculation, it was assumed that the immediate donor to ferredoxin does not contribute to the absorption change. Here we show that this assumption was incorrect as the differential absorption coefficient of (F_A, F_B) is about 2500 M^{-1} cm^{-1} at 480 nm. This value is fairly high as values around or less than 1000 M^{-1} cm^{-1} were often reported [see, e.g., Ke (1973)]. In the present work, the amplitudes

of the signals due to ferredoxin reduction are in fair agreement with complete electron transfer from PSI to ferredoxin.

The most striking observation of the present study is the presence of at least three first-order components of absorption changes ($t_{1/2} \approx 500$ ns, 20 μs and 100 μs) which are observed when soluble ferredoxin is added to isolated PSI or to cyanobacterial membranes containing mostly PSI. These kinetic components correspond presumably to electron transfer reactions within PSI–ferredoxin preformed complexes. The three phases were observed at 480 and 580 nm with various PSI–ferredoxin combinations. Their observation with *Synechocystis* membranes as well as with isolated PSI reaction centers most likely excludes the possibility that one or the other phase results from partial degradation of PSI. Moreover, the three phases were detected with dissolved crystals of PSI trimers from *Synechococcus* and with highly purified ferredoxin of two different origins. This general behavior strongly suggests that the observed kinetic complexity does not result from some heterogeneity of one or both partners. The decay-associated spectra of the different phases in the 460–600-nm region will be shown in a forthcoming paper. They are fully consistent with electron transfer from $(F_A, F_B)^-$ to ferredoxin.

The first question which arises is what species, besides ferredoxin, participate in one or several of the first-order kinetic components. F_A or F_B, or both, are certainly involved, but we will first discuss whether the secondary acceptors preceding (F_A, F_B) during electron transfer inside PSI could participate as well. These secondary acceptors are the phylloquinone A_1 and the [4Fe-4S] center F_X (Golbeck & Bryant, 1991). Flash-absorption changes in the UV region (Brettel, 1988; Sétif & Brettel, 1993) as well as time-resolved EPR spectroscopy (Bock et al., 1989) showed that A_1^- is transferring an electron to one of the iron–sulfur centers F_A, F_B, or F_X with a halftime of about 200 ns in cyanobacterial reaction centers. This implies that A_1 is most probably not involved in the reactions observed in the present study (except for the lag shown in Figure 3). This is corroborated by the observation that the three first-order phases are of small amplitude at 460 nm, in agreement with the fact that ferredoxin and its immediate donor(s) have similar differential absorption coefficients at this wavelength (not shown). The possible participation of F_X must be considered more seriously as the difference spectrum of the [4Fe-4S] center F_X is not expected to be much different from the difference spectrum of (F_A, F_B). If F_X is involved in the presently described reactions, this should be true in the case of the 500-ns phase, as F_X is preceding (F_A, F_B) in the electron transfer pathway inside PSI. We will discuss this possibility in view of the present knowledge of the PSI structure. The recently published X-ray structure of PSI (Krauss et al., 1993) showed that F_X is located well below the stromal surface of PSI. By using the electron density map of PSI and by trying to let ferredoxin come as close as possible to the different iron–sulfur centers of PSI, it is found that the minimal edge-to-edge distance between F_X and soluble ferredoxin is larger than 20 Å (P. Fromme, personal communication). A distance of 20 Å is not compatible with a submicrosecond electron transfer to ferredoxin. This can be checked by using the empirical formula derived by Moser and Dutton (1992):

$$\log k_{et} = 15 - 0.6R - 3.1(-\Delta G^\circ - \lambda)^2/\lambda$$

where k_{et} is the electron transfer rate in s^{-1}, R is the edge-to-edge distance (in Å) between the reactants, and ΔG° and λ are, respectively, the standard Gibbs free energy of reaction and the reorganization energy in eV. We estimated the maximum rate of electron transfer from F_X^- to ferredoxin to be 1.0×10^3 s^{-1} ($t_{1/2} = 690$ μs) by assuming $-\Delta G^\circ = \lambda$. The halftime thus calculated is certainly highly underestimated as the approximation $-\Delta G^\circ = \lambda$ probably does not hold. In spite of this underestimation, this halftime is three orders of magnitudes larger than 500 ns. It appears therefore very unlikely that F_X is involved in the fastest phase of ferredoxin reduction. This implies that the immediate donor to ferredoxin in the 500-ns reaction is either F_A or F_B and that this immediate donor is reduced within a time shorter than 500 ns. Such conclusions are in accordance with a former proposal that (F_A, F_B) is reduced with a halftime of 200 ns in cyanobacterial PSI (Sétif & Brettel, 1993).

The presence of three different first-order phases has to be explained assuming homogeneity of both PSI and ferredoxin and the participation of at most three species (F_A, F_B, and ferredoxin). For a kinetic system involving only first-order processes, the presence of three different species or states (reduced state of either F_A, F_B or ferredoxin) corresponds to two different exponential components describing the time evolution of the system (even if any state is kinetically coupled to all others). Therefore, the observation of three different components requires that the system under study is more complex. This complexity may arise either from some conformational transitions that are rate-limiting for ferredoxin reduction or from the existence of several types of PSI–ferredoxin complex. Conformational transitions appear rather unlikely as such transitions are expected to depend upon viscosity, contrary to what is observed for the three first-order components. Therefore, it is tentatively concluded that at least two and possibly three types of PSI–ferredoxin complex are present in order to account for the observed kinetic complexity of ferredoxin reduction. Further studies are necessary to choose between two or three types of complex and to understand the observed differences in the decay-associated spectra of the different components. Though speculative, the possible existence of geometrically distinct sites is compatible with the known structure of PSI. By the same approach as described above for F_X, the minimal edge-to-edge distances were found to be 15 and 11 Å between ferredoxin and, respectively, F_I (either F_A or F_B, the farthermost from the stromal surface of PSI) and F_{II} (the closest to the stromal surface) (P. Fromme, personal communication). These minimal distances correspond to two well-separated sites. In one of these, ferredoxin would be closer to F_I, whereas it would be closer to F_{II} in the other one.

ACKNOWLEDGMENT

We thank Dr. P. Fromme for providing us crystals of PSI trimers from *Synechococcus* and from unpublished observations concerning the closest distance of approach of ferredoxin from PSI, Dr. M. Rögner for the gift of PSI trimers from *Synechocystis* 6803, for his advice for preparing monomers and trimers of PSI, and for sending us a preprint of his work. We also thank Dr. J.-P. Jacquot for providing us ferredoxin from *Chlamydomonas*, Dr. B. Lagoutte for preparing membranes from *Synechocystis*, and C. Lelong for the preparation of ferredoxin from *Synechocystis*.

REFERENCES

Andersen, B., Koch, B., & Scheller, H. V. (1992a) *Physiol. Plant. 84*, 154–161.

Andersen, B., Scheller, H. V., & Møller, B. L. (1992b) *FEBS Lett. 311*, 169–173.

Arnon, D. I. (1949) *Plant Physiol. 24*, 1–15.

Bald, D., Kruip, J., Boekema, E. J., & Rögner, M. (1992) in *Research in Photosynthesis* (Murata, N., Ed.) Vol. I, pp 629–632, Kluwer Academic Publishers, Dordrecht, The Netherlands.

Bock, C. H., van der Est, A. J., Brettel, K., & Stehlik, D. (1989) *FEBS Lett. 247*, 91–96.

Bottin, H., & Mathis, P. (1985) *Biochemistry 24*, 6453–6460.

Bottin, H., & Lagoutte, B. (1992) *Biochim. Biophys. Acta 1101*, 48–56.

Bouges-Bocquet, B. (1980) *Biochim. Biophys. Acta 590*, 223–233.

Brettel, K. (1988) *FEBS Lett. 239*, 93–98.

Chen, L., Durley, R., Poliks, B. J., Hamada, K., Chen, Z., Mathews, F. S., Davidson, V. L., Satow, Y., Huizinga, E., Vellieux, F. M. D., & Hol, W. G. J. (1992) *Biochemistry 31*, 4959–4964.

Fee, J. A., & Palmer, G. (1971) *Biochim. Biophys. Acta 245*, 175–195.

Gekko, K., & Timasheff, S. N. (1981) *Biochemistry 20*, 4667–4676.

Golbeck, J. H., & Bryant, D. A. (1991) in *Current Topics in Bioenergetics* (Govindjee, Ed.) pp 83–177, Academic Press, London.

Hervas, M., Navarro, J. A., & Tollin, G. (1992) *Photochem. Photobiol. 56*, 319–324.

Hervas, M., Ortega, J. M., Navarro, J. A., De la Rosa, M. A., & Bottin, H. (1994) *Biochim. Biophys. Acta 1184*, 235–241.

Hurley, J. K., Salamon, Z., Meyer, T. E., Fitch, J. C., Cusanovich, M. A., Markley, J. L., Cheng, H., Xia, B., Chae, Y. K., Medina, M., Gomez-Moreno, C., & Tollin, G. (1993) *Biochemistry 32*, 9346–9354.

Jacobson, B. L., Chae, Y. K., Markley, J. L., Rayment, I., & Holden, H. M. (1993) *Biochemistry 32*, 6788–6793.

Ke, B. (1973) *Biochim. Biophys. Acta 301*, 1–33.

Knaff, D. B., & Hirasawa, M. (1991) *Biochim. Biophys. Acta 1056*, 93–125.

Krauss, N., Hinrichs, W., Witt, I., Fromme, P., Pritzkow, W., Dauter, Z., Betzel, C., Wilson, K. S., Witt, H. T., & Saenger, W. (1993) *Nature 361*, 326–330.

Lelong, C., Sétif, P., Lagoutte, B., & Bottin, H. (1994) *J. Biol. Chem. 269*, 10034–10039.

Mathis, P., & Sétif, P. (1981) *Isr. J. Chem. 21*, 316–320.

Moser, C. C., & Dutton, P. L. (1992) *Biochim. Biophys. Acta 1101*, 171–176.

Pelletier, H., & Kraut, J. (1992) *Science 258*, 1748–1755.

Rögner, M., Nixon, P. J., & Diner, B. A. (1990) *J. Biol. Chem. 265*, 6189–6196.

Rousseau, F., Sétif, P., & Lagoutte, B. (1993) *EMBO J. 12*, 1755–1765.

Rypniewski, W. R., Breiter, D. R., Benning, M. M., Wesenberg, G., Oh, B.-H., Markley, J. L., Rayment, I., & Holden, H. M. (1991) *Biochemistry 30*, 4126–4131.

Schmitter, J.-M., Jacquot, J.-P., de Lamotte-Guéry, F., Beauvallet, C., Dutka, S., Gadal, P., & Decottignies, P. (1988) *Eur. J. Biochem. 172*, 405–412.

Sétif, P., & Brettel, K. (1993) *Biochemistry 32*, 7846–7854.

Sonoike, K., Hatanaka, H., & Satoh, S. (1993) *Biochim. Biophys. Acta 1141*, 52–57.

Tagawa, K., & Arnon, D. I. (1968) *Biochim. Biophys. Acta 153*, 602–613.

Tiede, D. M., Vashishta, A.-C., & Gunner, M. R. (1993) *Biochemistry 32*, 4515–4531.

Timasheff, S. N., & Arakawa, T. (1989) in *Protein Structure, a practical approach* (Creighton, T. E., Ed.) pp 331–345, IRL Press, Oxford.

Tsukihara, T., Fukuyama, K., Nakamura, M., Katsube, Y., Tanaka, N., Kakudo, M., Wada, K., Hase, T., & Matsubara, H. (1981) *J. Biochem. (Tokyo) 90*, 1763–1773.

Tsukihara, T., Fukuyama, K., Mizushima, M., Harioka, T., Kusunoki, M., Katsube, Y., Hase, T., & Matsubara, H. (1990) *J. Mol. Biol. 216*, 399–410.

Venturoli, G., Mallardi, A., & Mathis, P. (1993) *Biochemistry 32*, 13245–13253.

Zanetti, G., & Merati, G. (1987) *Eur. J. Biochem. 169*, 143–146.

Zilber, A. L., & Malkin, R. (1988) *Plant Physiol. 88*, 810–814.

Witt, H. T., Krauss, N., Hinrichs, W., Witt, I., Fromme, P., & Saenger, W. (1992) in *Research in Photosynthesis* (Murata, N., Ed.) Vol. I, pp 521–528, Kluwer Academic Publishers, Dordrecht, The Netherlands.